RSC Advances

Solvent treatment effect of the PEDOT:PSS anode interlayer in inverted planar perovskite solar cells

Journal:	*RSC Advances*
Manuscript ID	RA-ART-12-2015-025787.R1
Article Type:	Paper
Date Submitted by the Author:	28-Jan-2016

Complete List of Authors:	Li, Xue-Yuan; Suzhou Institute of Nano-Tech and Nano-Bionics, Chinese Academy of Sciences, Printable Electronic Research Center Zhang, Liangping; Suzhou Institute of Nano-Tech and Nano-Bionics, Chinese Academy of Sciences, Printable Electronic Research Center Tang, Feng; Suzhou Institute of Nanotech and Nanobionics, i-Lab Bao, Zhongmin; Soochow University, Institute of Functional Nano & Soft Materials Lin, jian; Suzhou Institute of Nano-tech and Nano-bionics, Printable Electronic Research Center Li, Yanqing; Soochow University, Institute of Functional Nano & Soft Materials Chen, Liwei; Suzhou Institute of Nanotech and Nanobionics, i-Lab Ma, Changqi; Suzhou Institute of Nano-Tech and Nano-Bionics, Chinese Academy of Sciences, Printable Electronics Research Center
Subject area & keyword:	Solar energy < Energy

Journal Name

ARTICLE

Solvent treatment effect of the PEDOT:PSS anode interlayer in inverted planar perovskite solar cells

Received 00th January 20xx,
Accepted 00th January 20xx

DOI: 10.1039/x0xx00000x

www.rsc.org/

Xue-Yuan Li,[a), d)] Lian-Ping Zhang,[a)] Feng Tang,[b)] Zhong-Min Bao,[c)] Jian Lin,[a)] Yan-Qing Li,[c)] Liwei Chen,[b)] Chang-Qi Ma[a),*]

Inverted planar perovskite (PVSK) solar cells with a device structure of ITO/PEDOT:PSS/PVSK/$PC_{61}BM$/Al have emerged as a new generation solar cells owing to their advantages of high power conversion efficiency (PCE), low processing temperature and potential low cost. In this paper, polar solvent treatment effect of the PEDOT:PSS anode interlayer on PVSK solar cell performance was investigated. The conductivity of PEDOT:PSS film was found to increase by washing with polar solvents, including H_2O, ethanol (EtOH), and a mixture solvent of ethanol and H_2O (EtOH:H_2O = 8:2 v/v), which was attributed to the removal of PSS component from the PEDOT:PSS film, leading to a PEDOT-rich surface. However, PCE of perovskite solar cells decreased from 9.39% of the pristine PEDOT:PSS film based device to 4.21%, 8.35%, 7.13% for the H_2O-, EtOH- and EtOH:H_2O treated PEDOT:PSS film based devices, respectively, suggesting that high conductivity of the PEDOT:PSS film does not ensure a high device performance of the inverted PVSK solar cells. UV-vis absorption spectra, AFM surface morphology and SEM images of the PVSK films deposited on different PEDOT:PSS surface were studied, and results showed that PEDOT-rich surface is not favorable for the crystal growth of PVSK layer, and consequently leads to poor device performances. This conclusion was further supported by the improved device performance of PVSK solar cells based on PEDOT:PSS/PSSNa anode buffer layer, where an additional poly(sodium p-styrenesulfonate) (PSSNa) layer was deposited on PEOT:PSS surface.

1. Introduction

Organo-lead-halide perovskite (PVSK) materials have recently attracted tremendous attentions in photovoltaic application due to their intensive solar light absorption ability, low non-radiative carrier recombination rates, and ease of device fabrication.[1] Power conversion efficiency (PCE) of PVSK solar cells has been boosting from 3.8%[2] to more than 20%[3] in the past few years. Historically, PVSK solar cell derived from mesoporous dye-sensitized solar cells,[4] however, various types of PVSK solar cells with different device structure have been developed up to now, including TiO_2 based meso-structure,[4] TiO_2 based planar structure[5] and poly(3,4-ethylene-dioxythiophene):poly(styrene sulfonate) (PEDOT:PSS) based inverted planar structure.[6-9] In comparison with the conventional mesoporous type perovskite solar cells, the PEDOT:PSS based inverted planar perovskite solar cells (IP-PVSK) have advantages of ease of fabrication, low processing temperature and good compatibility with roll to roll processing. To date, high power conversion efficiency of 18% has been achieved in IP-PVSK solar cells.[10]

In organic/polymer solar cells, the influence of the solvent treatment on PEDOT:PSS films on the photovoltaic performance have been widely investigated. Results showed that conductivity of the PEDOT:PSS films could be enhanced by washing with polar solvents, such as H_2O, ethanol etc., and such solvent treated PEDOT:PSS film could serve as transparent electrode in organic/polymer solar cells.[11-13] For PVSK solar cells, it has been demonstrated that the composition and property of the underlying layer plays an important role in influencing the crystal growth of the perovskite film, and consequently limiting the PVSK solar cell performance.[14, 15] Very recently, Ouyang *et al*. demonstrated that the electronic properties of the PEDOT:PSS layer was greatly influenced by the deposition of the perovskite precursor solution and consequently effected the device performance of the perovskite solar cells.[9] However, the influence of solvent treatment of the PEDOT:PSS layer on the PVSK solar cell performance has not been reported yet.

Aiming to understanding the solvent treatment effect of PEDOT:PSS anode buffer layer on solar cell performance, PVSK solar cells based on solvent-treated PEDOT:PSS films were fabricated and tested in this paper. The conductivity, optical property, and surface morphology of the solvent-treated

[a.] *Printable Electronics Research Centre, Suzhou Institute of Nano-Tech and Nano-Bionics, Chinese Academy of Sciences, Collaborative Innovation Center of Suzhou Nano Science and Technology, No. 398 Ruoshui Road, SEID, SIP, Suzhou, Jiangsu, 215123, PR China, Email: cqma2011@sinano.ac.cn.*

[b.] *i-Lab, Suzhou Institute of Nano-Tech and Nano-Bionics, Chinese Academy of Sciences, Collaborative Innovation Center of Suzhou Nano Science and Technology, No. 398 Ruoshui Road, SEID, SIP, Suzhou, Jiangsu, 215123, PR China.*

[c.] *Institute of Functional Nano & Soft Materials, Soochow University, Collaborative Innovation Center of Suzhou Nano Science and Technology, No. 199 Renai Road, SEID, SIP, Suzhou Jiangsu 215123, PR China.*

[d.] *University of China Academy of Sciences, Beijing 100049, China.*

Electronic supplementary information (ESI) available. Se

PEDOT:PSS films, as well as the crystallinity and morphology of the perovskite films deposited on these solvent-treated PEDOT:PSS films were investigated carefully. Results showed that the PSS-rich surface is helpful to achieve high performance PVSK solar cells, whereas solvent-treated PEDOT:PSS films, which have a PEDOT-rich surface, is not favorable for the crystal growth of perovskite film, and leading to poorer device performance. The current work provides an important guideline for the development of high performance IP-PVSK solar cells.

2.Experimental

2.1 Materials and preparation

Poly(3,4-ethylenedioxythiophene):poly(styrene sulfonate) (PEDOT:PSS Clevios PVP AI 4083) was purchased from Heraeus Precious Metals GmbH & Co. KG. Phenyl-C_{61}-butyric acid methyl ester ($PC_{61}BM$) was purchased from Solenne B.V. Poly(sodium p-styrenesulfonate) (PSSNa, Mn=70,000 g/mol) was purchased from Acros Organics. $PbCl_2$ (99%), CH_3NH_2 (32 wt% in absolute ethanol), HI (30% in water) were purchased from Sinopharm Group Co. Ltd. and used as received. Methylammonium iodide (MAI) was synthesized according to the literature.[16]

2.2 PEDOT:PSS films preparation and characterization

The PEDOT:PSS films for UV-Vis absorption, AFM morphology, and conductivity measurement were prepared by spin-coating the Clevios 4083 solution on quartz glass. These films were baked at 124 ºC for 30 min inside the glove box. After that, 100 µL solvent (H_2O, ethanol, or ethanol-H_2O mixture (8:2, v/v)) was dropped onto the dried PEODT:PSS film and then spin-casting at 3000 rpm for 60 s in air. These solvent-treated PEDOT:PSS films were further dried at 140 ºC for 5 min in the ambient before measurement. To make sure that all these solvent-treated PEDOT:PSS films have similar layer thickness, the layer thickness of the initial PEDOT:PSS films for solvent treatment were adjusted by changing the spin speed until similar final layer thickness of ~35 nm was achieved after solvent treatment (see more details in Supporting Information). As for the films for the conductivity measurement, much thicker PEDOT:PSS films (around 120 nm) were prepared to provide a better measurement accuracy.

The layer thickness of the PEDOT:PSS films was measured using an AlphaStep profilometer (Veeco, Dektak 150). Conductivity of PEDOT:PSS film (ρ) was calculated according to the following formulation: $\rho = Rs \cdot d$, where Rs and d represent the sheet resistance and the thickness of measured film, respectively. Rs was measured by a four-point probe method with a Keithley Instruments Model 4200-SCS. To minimize the effect of the contact resistance between the PEDOT:PSS film and the probe, 200 nm thick aluminum layer was thermal deposited on the PEDOT:PSS surface as top electrode. The UV-vis absorption spectra were recorded with a Lamada 750 UV/vis/NIR spectro-photometer (PerkinElmer). Atomic Force Microscopy (AFM) images were recorded by VEECO Dimension 3100. The scanning electron microscopy (SEM) images were obtained using an HITACHI S4800 scanning electron microscope. XPS experiments were carried out in a Kratos AXIS UltraDLD ultrahigh vacuum (UHV) surface analysis system, consisting of a multiport carousel chamber, a deposition chamber, and an analysis chamber. Base pressures in the three chambers are better than 5×10^{-10}, 5×10^{-10}, and 3×10^{-10} Torr, respectively. A monochromatic aluminum Kα source (1486.6 eV) was used in the XPS measurements to study the interfacial chemical states. All measurements were performed at room temperature. The photo-electrons were collected by a hemispherical analyzer with a total instrumental energy resolution of 0.5 eV for the XPS measurements. The contact angle between DMF, H_2O or CH_2I_2 on various PEDOT:PSS surface was measured by an contact angle meter Model SL150 (USA KINO Industry). 30 seconds delay was performed to stabilize the contact between the solvent and PEDOT:PSS film, and a circling fitting mode was used to fit the contact angle.

2.3. Solar cell fabrication and testing

Patterned ITO glass substrates were subsequently cleaned by ultrasonic in surfactant aqueous solution, deionized water, acetone twice, and isopropyl alcohol for 30 min each. After nitrogen blow drying, the substrates were explored in UV/ozone for 30 min. A thin PEDOT:PSS film (~35 nm) was deposited according to the method described in section 2.2. For the perovskite ($CH_3NH_3PbI_{3-x}Cl_x$) layer, a precursor solution of CH_3NH_3I and $PbCl_2$ (mol/mol=3/1) in anhydrous DMF (0.6 M) was spin-coated onto the as-prepared PEDOT:PSS layer at 6000 rpm for 60 sec and then annealed at 95 ºC for 70 min inside the glove box. Note that concentration of PVSK precursor solution was optimized in our lab, which leads to a thinner PVSK film than that reported in the literature (*vide infra*). After that, a solution of PCBM in chlorobenzene (20 mg/mL) was spin-casted onto the perovskite film at 1000 rpm for 60 s to form a 60 nm thin film. Finally, a 100 nm Al layer was deposited under 1×10^{-4} Pa via thermal evaporation through a mask to ensure an effective area of 16 mm^2 or 9 mm^2 of the devices. The current density-voltage (*J-V*) measurement was carried out inside the glove box with a Keithley 2400 source meter under simulated AM 1.5G solar illumination (100 mW/cm^2) generated by white light from halogentungsten lamp, filtered by a UV filter and a Hoya LB120 daylight blue filter.[17] External quantum efficiencies (EQE) were measured under simulated one sun operation conditions using bias light from a 532 nm solid state laser (Changchun New Industries, MGL-III-532). Light from a 150 W tungsten halogen lamp (Osram 64642) was used as probe light and modulated with a mechanical chopper before passing the monochromator (Zolix, Omni-λ300) to select the wavelength. The response was recorded as the voltage by an I-V converter (QE-IV Convertor, Suzhou D&R Instruments), using a lock-in amplifier (Stanford Research Systems SR 830). A calibrated Si cell was used as reference. The test device was kept behind a quartz window in a nitrogen filled container during the EQE measurement.

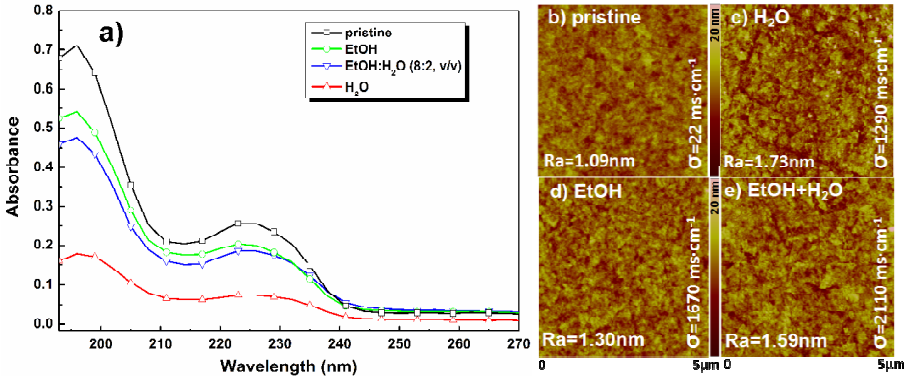

Figure 1. UV-Vis absorption spectra (a) and AFM surface topology images (b-e) of the pristine and solvent treated PEDOT:PSS films (35 ± 5 nm) deposited on quartz glass. For the AFM surface topology images, the high scale is 20 nm, and the scan area is 5 μm × 5 μm. The conductivity (σ) of thick PEDOT:PSS films (120 ± 13 nm) measured by a four-point probe method is also listed in the corresponding AFM image.

3. Results and discussion

3.1 Influence of solvent treatment on the conductivity and surface properties of PEDOT:PSS films

Figure 1 shows the UV-Vis absorption spectra and AFM surface morphology images of the pristine and solvent treated PEDOT:PSS films. As can be seen from Figure 1a, the pristine PEDOT:PSS film showed two absorption bands peaking at 196 and 225 nm, which were attributed to the absorption of PSS component.[11, 12, 18] Clearly, the absorption intensity of these peaks decreased for the solvent treated films. Note that all these films for UV-Vis absorption measurement have similar layer thickness (35 ± 5 nm). The decrease of absorption intensity was therefore not attributed to the decrease of the PEDOT:PSS layer thickness but to the decrease of PSS content in these films. The measured conductivity of the PEDOT:PSS film increased from 22 mS·cm^{-1} for the pristine film,[19, 20] to 1290, 1670 and 2110 mS·cm^{-1} for the H_2O, EtOH and EtOH:H_2O treated films, respectively (see Figure 1). In the meanwhile, AFM surface imaging (Figure 1 b-e) showed the roughness of the PEDOT:PSS films increased slightly from 1.09 nm for the pristine PEDOT:PSS film to 1.3-1.7 nm for the solvent treated ones, confirming that surface property of the PEDOT:PSS film changed greatly by such solvent treatment. Such a conductivity improvement and surface morphology changes were also reported in the literatures, and was ascribed the removal of PSS component during the solvent processing.[11, 12, 18]

To further confirm that PSS component was partially removed by solvent treatment, X-ray photoelectron spectroscopy (XPS) was utilized to determine the surface composition of the prepared PEDOT:PSS films. **Figure 2** shows the XPS spectra of the pristine and solvent treated PEDOT:PSS films. As can be seen here, all these PEDOT:PSS films showed

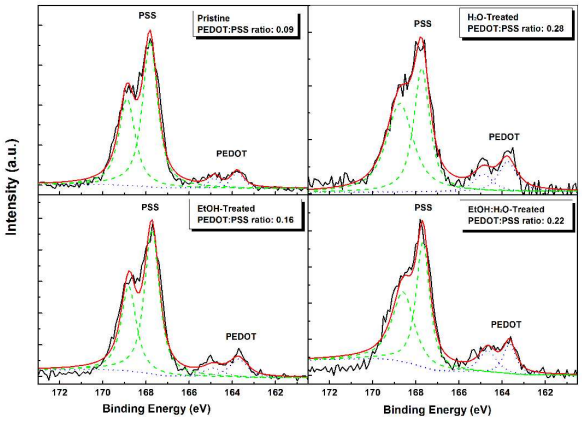

Figure 2. S (2p) core level spectra for pristine and solvent treated PEDOT:PSS films. The PEDOT:PSS ratios determined from the relative integral area of peak at 163.5 eV and 167.5 eV are listed in each figure.

two signed peak regions at 170-166 and 166-163 eV, which are corresponding to S(2p) of PSS and PEDOT moieties, respectively.[21] The PEDOT:PSS ratio of the thin films, determined by the relative integral area of peaks at 163.5 eV and 167.5 eV, respectively, was increased from 0.09 for the pristine PEDOT:PSS film, to 0.28 for H_2O-treated film, 0.16 for EtOH treated film, and 0.22 for EtOH:H_2O-treated film, respectively, suggesting a more PEDOT-rich surface formed for these solvent-treated PEDOT:PSS films. For comparison, PEDOT:PSS/PSSNa film, where an additional poly(sodium p-styrenesulfonate) (PSSNa) layer was spun costed on the H_2O-treated PEDOT:PSS surface was also fabricated and tested. **Figure S1** (in supporting information) shows the UV-vis and XPS of this PEDOT:PSS/PSSNa film. As can be seen here, after deposition of an additional PSSNa layer, the absorption

intensity at 196 and 225 nm increased greatly when compared to that of H_2O-treated PEDOT:PSS film, suggesting that PSSNa was successfully deposited on PEDOT:PSS surface. In addition, only PSS component can be found in XPS spectrum (Figure S1b), unambiguously confirming that a PSS-rich surface formed on this PEDOT:PSS/PSSNa surface.

To further confirm the surface property change of these PEDOT:PSS films, the contact angles between the pristine and solvent-treated PEDOT:PSS films with DMF, H_2O or CH_2I_2 solvent were tested. Unfortunately, DMF and H_2O were found to be able to penetrate into the PEDOT:PSS film, and it is not possible to get an equilibrium state for the contact angle measurement. This could be understood by the fact that PEDOT:PSS is highly dispersed in DMF and H_2O. However, hydrophobic CH_2I_2 is able to form a stable droplet on the PEDOT:PSS surface, and the contact angels were measured to be 36.4° for the pristine PEDOT:PSS film, and 33.7°, 32.1°, 32.4°, and 41.0° for the H_2O-, EtOH-, EtOH:H_2O-treated PEDOT:PSS film and PEDOT:PSS/PSSNa film surface (Figure S2 in supporting information). The contact angle measurement results clearly showed that more hydrophobic surface formed after being treated with polar solvent, whereas hydrophilic surface formed after deposition of PSSNa. Together with the UV-Vis and XPS results, one can conclude that H_2O, EtOH and EtOH-H_2O treated PEDOT:PSS surface are PEDOT-rich surface owing to the removal of PSS by washing with solvents,[11, 12, 18] whereas PEDOT:PSS/PSSNa surface is more hydrophilic for the high PSS content on the surface.

3.2 Perovskite thin film qualities on various PEDOT:PSS surface

Perovskite films were then deposited on the pristine and solvent-treated PEDOT:PSS surfaces by spin-coating the precursor solution and the following thermal annealing. For comparison, perovskite film on PEDOT:PSS/PSSNa surface was also prepared and tested. The surface morphology of these films were investigated by scanning electron microscope (SEM) and atomic force microscope (AFM). **Figure 3** shows the top-view SEM, cross-section SEM and AFM surface topology images of the perovskite films. As shown in Figure 3a1, the perovskite film deposited on the pristine PEDOT:PSS showed reasonable condensed crystalline film with few small pin holes. AFM image (Figure 3a3) confirmed a surface roughness of 10.7 nm for this film. The PVSK layer thickness was found to decrease slightly (less than 10%) for those PVSK films deposited on solvent-treated PEDOT:PSS film (see cross sectional SEM images). In addition, much rougher surface was found for those PVSK film deposited on the solvent treated PEDOT:PSS films (AFM images in Figure 3 b3-d3), among which the H_2O-treated PEDOT:PSS film based PVSK film showed a roughest surface (MRS = 16.5 nm) and large pin holes (Figure 3b). Slightly increased surface roughness was found for PVSK films deposited on EtOH and EtOH:H_2O mixture treated PEDOT:PSS film (RMS = 12.2 and 12.8 nm, respectively), and reasonable condense PVSK film formed, suggesting that EtOH containing solvent treated PEDOT:PSS surface has less effect on the crystallinity of the PVSK films than H_2O-only solvent. In contrast, PVSK film

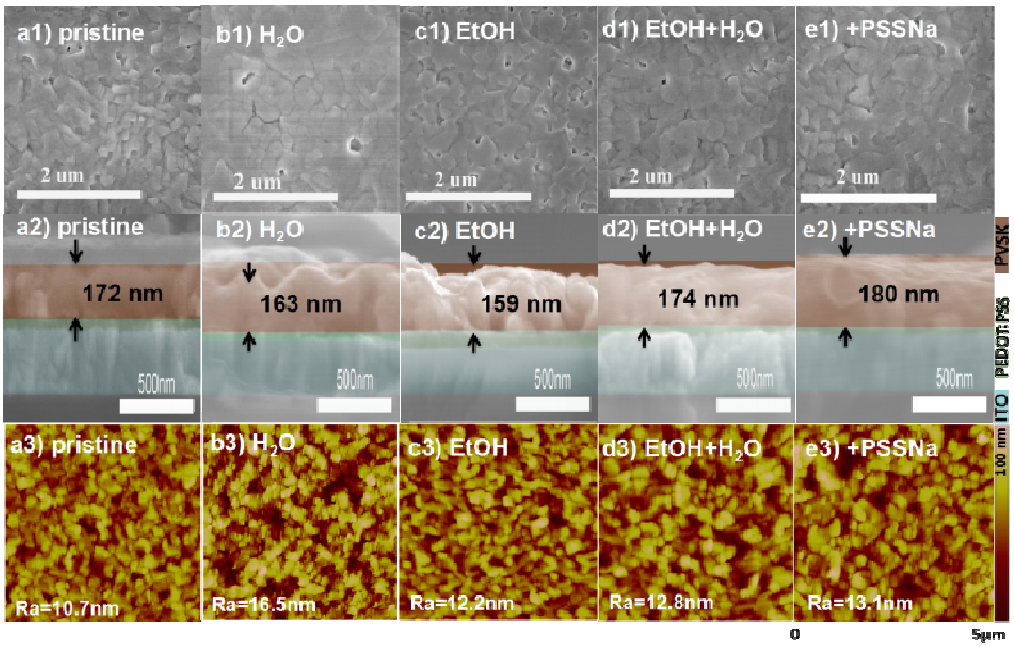

Figure 3. Top-view SEM (a1-e1), cross-sectional SEM images (a2-e2) and AFM surface topology images (a3-e3) of the perovskite layer based on pristine (a); H_2O treated (b); EtOH treated (c); EtOH+H_2O (8:2,v/v, d) treated(d); additional PSSNa on H_2O treated PEDOT:PSS films.

Journal Name

ARTICLE

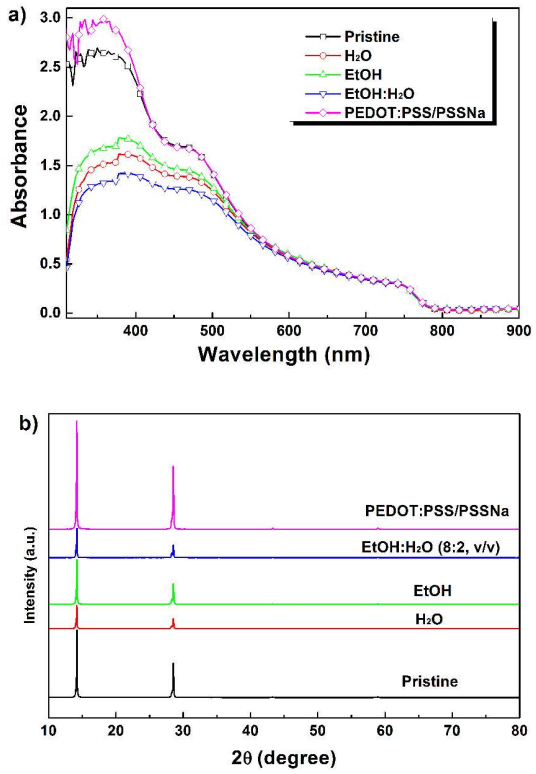

Figure 4. a): UV-Vis absorption spectra; b): X-ray diffraction patterns of perovskite layers based on pristine, H_2O-, EtOH-, EtOH:H_2O mixture- (8:2,v/v) treated PEDOT:PSS films, and on PEDOT:PSS/PSSNa surface.

deposited on PEDOT:PSS/PSSNa surface showed more homogeneous film with larger and more condensed crystal domains (Figure 3e1 and e2), suggesting a better perovskite thin film morphology was obtained on the PEDOT:PSS/PSSNa surface.

UV-Vis absorption spectra (**Figure 4a**) and X-ray diffraction (**Figure 4b**) were applied to further study the quality of the perovskite films. As can be seen from Figure 4a, PVSK film on the pristine PEDOT:PSS showed a broad absorption band over 300-800 nm, which is similar to that reported in the literatures.[22] The absorption intensity (over 300-500 nm) decreased for the PVSK film deposited on the solvent treated PEDOT:PSS films. Since the layer thicknesses of these PVSK films are all around 170 nm (Figure 3a2-d2), such an absorption decrease was attributed to the decrease of the thin film quality of PVSK films, rather than to the PVSK layer thickness. The PVSK crystal quality was further checked with XRD measurements. Figure 4b shows the XRD patterns of the PVSK films deposited on various PEDOT:PSS surface. As can be seen here, all these films showed typical diffraction peaks of PVSK film at 2θ of 14.1°, 28.4°, 43.1°, 58.7°, respectively.[23, 24] However, the intensity of the diffraction peak decreased for perovskite film deposited on solvent treated PEDOT:PSS film, demonstrating a decrease of crystalline property of the perovskite films, which is in good accordance with the SEM and AFM results.

Not surprisingly, higher UV-vis absorption intensity over 300-400 nm (Figure 4a) and more intensive XRD diffraction peaks (Figure 4b) were found for the PVSK film deposited on PEDOT:PSS/PSSNa surface, confirming that improved PVSK thin film quality was obtained on PEDOT:PSS/PSSNa film. Knowing that perovskite film defects can be passivated by the amine group[25] or other hetero atoms[26] owing to the complexation ability of hetero atom with Pd anion, it is reasonable to speculate that PSS molecules are dispersed in the PVSK film when dropping the PVSK precursor solution onto the PEDOT:PSS surface. The oxygen anions of the sulfonic groups of PSS would passivate the boundary defect of the perovskite film through a Pd-O bond during the crystal growth of perovskite film, and consequently improve PVSK film quality. For those solvent-treated PEDOT:PSS film, since PSS moiety was partially removed by solvent-treatment, such a PSS passivation effect was limited, and consequently led to poor PVSK thin film quality. However, more experiments are still needed to fully confirm the interaction between PSS and PVSK film. Nevertheless, it is clear that PSS-rich surface is helpful in improving perovskite thin film quality, whereas PEDOT-rich surface is not favorable for the crystal growth of perovskite film and leads to poor thin film quality.

3.3 Performances of devices based on solvent-treated PEDOT: PSS layer

To further understand the influence of solvent treatment of the PEDOT:PSS film on PVSK solar cell performance, inverted planar heterojunction perovskite solar cells with a structure of ITO/PEDOT:PSS/PVSK/$PC_{61}BM$/Al were fabricated and tested, where various solvent treated PEDOT:PSS layer was used as the hole transporting layer. **Figure 5** shows the *J-V* curves and EQE spectra of these PVSK solar cells. The PV performance data are summarized in **Table 1** and the statistics diagram of these devices are shown in **Figure 6**. As can be seen here, the pristine PEDOT:PSS film based device gave an open circuit voltage (V_{OC}) of 0.89 V, a short circuit current (J_{sc}) of 17.6 mA/cm^2, a fill factor (FF) of 0.61 and an overall power conversion efficiency (PCE) of 9.65%. The achieved PCE is slightly lower that reported in the literatures,[8, 16, 27] but still

reasonable for PVSK device with a PVSK layer thickness of 170 nm (Figure 3, SEM cross section). Surprisingly, although the conductivity of the PEDOT:PSS film was improved by solvent treatment, devices based on the such solvent treated PEDOT:PSS films gave also poorer device performance and worst performance reproducibility than the reference cell (Table 1 and Figure 6). The decreased device performance for the H_2O- treated PEDOT:PSS based device is mainly due to the low open-circuit voltage (V_{OC} = 0.65 V, Table 1). Although the detailed reason for V_{OC} decrease is not clear yet, the rougher PVSK surface that leading to worse surface coverage of $PC_{61}BM$ was supposed to be the main reason. Short circuit (J_{SC}) and fill factor (FF), on the other hand, are found to be slightly decreased after the PEDOT:PSS surface treatment with H_2O. Less negative effect was found for EtOH based solvents (Figure 6 and Table 1, entry 3 and 4), which is in good accordance to less effect on the crystal thin film (SEM results, Figure 3). EQE spectra showed that all these PVSK device have high photon-electron conversion efficiency over 350-750 nm. Slight EQE variation for different cells was found, which could be due to layer thickness difference for different devices. This result demonstrated that PVSK device performance was more direct related to the PVSK thin film quality rather than to the conductivity of the PEDOT:PSS layer (hole transporting layer).

To further confirm that PSS is necessary to achieve high performance for PEDOT:PSS based inverted perovskite solar cells, devices with a structure of ITO/PEDOT:PSS/PSSNa/PVSK/$PC_{61}BM$/Al were fabricated and tested (Entry 5 in Table 1). The *J-V* cure and EQE curve of this PEDOT:PSS/PSSNa based device are shown in Figure 5a and 5b, respectively. As can be seen here, although J_{sc} (17.56 mA/cm^2) and FF (0.62) do not improved too much for this PSSNa layer associated device, the device performance was greatly improved owing to an improvement of V_{OC} to 0.93 V, yielding an overall PCE of 10.27%, which is even higher than that of the reference cell (Entry 1, Table 1). With that, one can conclude that PSS-rich surface is helpful in achieving high quality perovskite thin film, and the consequence device performance. However, for those solvent-treated PEDOT:PSS film, the PEDOT-rich surface leads to poorer perovskite thin film quality, and lower device performance was obtained for these solvent-treated PEDOT:PSS film, although conductivity of these films is improved by solvent treatment.

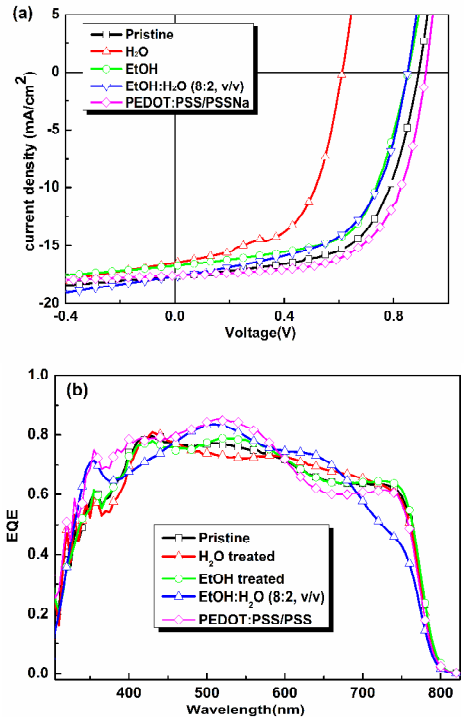

Figure 5. a) J-V curves and b) EQE spectra of inverted planar PVSK solar cells based on different PEDOT: PSS films. Device structure: ITO/PEDOT:PSS/PVSK/PCBM/Al

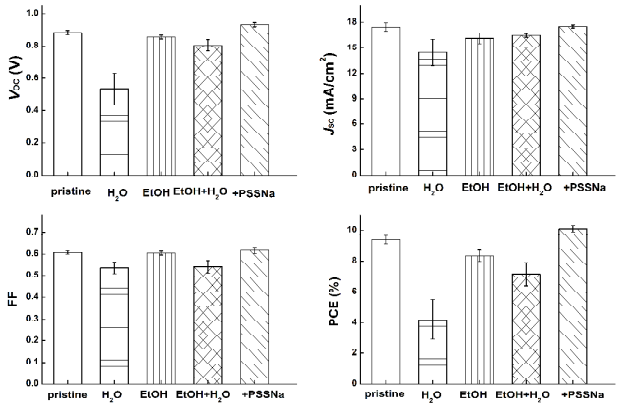

Figure 6. Statistics dates of PSCs devices of the pristine PEDOT: PSS and treated with H_2O, EtOH, EtOH:H_2O (v:v=8:2), and PEDOT:PSS/PSSNA.

Table 1. Photovoltaic performances of the best PVSK solar cells based on different PEDOT:PSS films

Entry	PEDOT:PSS layer treatment	Jsc[a] [mA/cm^2]	Voc [V]	FF	PCE[b] [%]	Ave. PCE[c] [%]
1	------	17.68	0.89	0.61	9.65	9.39±0.26
2	H_2O	16.52	0.61	0.57	5.73	4.21±1.29
3	EtOH	16.78	0.85	0.62	8.85	8.35±0.37
4	EtOH:H_2O (8:2, v/v)	17.69	0.85	0.57	8.64	7.13±0.75
5	Entry 2 + additional PSSNa layer	17.56	0.93	0.62	10.27	10.01±0.19

a: JSC was calculated by integrating the EQE spectrum with the AM 1.5G spectrum; b: PCE = V_{OC} ×J_{SC} ×FF; c: mean device PCE over 8 individual devices

4.Conclusions

In summary, we have systematically studied the influence of solvent treatment on the properties of the PEDOT:PSS films, the subsequent perovskite thin films as well as the PVSK solar cell performance. UV-Vis absorption and XPS analysis confirmed that PSS component was partially removed by washing with H_2O, EtOH or EtOH:H_2O (8:2, v/v), leading to a PEDOT-rich surface with an enhanced conductivity. UV-vis absorption spectra and XRD diffraction patterns analyses confirmed that perovskite film deposited on PSS-rich surface has better crystal quality, while decreased thin film quality was found for those perovskite film deposited on solvent treated PEDOT:PSS surface. Although the conductivity of PEDOT:PSS films was improved by solvent treatment, perovskite solar cell performance decreased in those solvent treated PEDOT:PSS film based device, demonstrating that PVSK solar cell performance is more related to the quality of PVSK film rather than the conductivity of the hole transporting layer. Interestingly, an additional PSSNa layer could improve device performance, suggesting that making a PSS-rich surface would be a feasible way to improve the performance of polymer buffer layer based PVSK solar cells.

Acknowledgment

The work is financially supported by Jiangsu Province Natural and Science Foundation, Department of Key Research and Development Plan (Grant No: BE2015071), and Strategic Priority Research Program of the Chinese Academy of Sciences (Grant No. XDA09020201).

References

1. M. A. Green, A. Ho-Baillie and H. J. Snaith, *Nat. Photonics*, 2014, **8**, 506-514.
2. A. Kojima, K. Teshima, Y. Shirai and T. Miyasaka, *J. Am. Chem. Soc.*, 2009, **131**, 6050-6051.
3. W. S. Yang, J. H. Noh, N. J. Jeon, Y. C. Kim, S. Ryu, J. Seo and S. I. Seok, *Science*, 2015, **348**, 1234-1237
4. M. M. Lee, J. Teuscher, T. Miyasaka, T. N. Murakami and H. J. Snaith, *Science*, 2012, **338**, 643-647.
5. K. Wojciechowski, M. Saliba, T. Leijtens, A. Abate and H. J. Snaith, *Energy Environ. Sci.*, 2014, **7**, 1142-1147.
6. S. Bai, Z. Wu, X. Wu, Y. Jin, N. Zhao, Z. Chen, Q. Mei, X. Wang, Z. Ye, T. Song, R. Liu, S.-t. Lee and B. Sun, *Nano Res.*, 2014, **7**, 1749-1758.
7. C.-W. Chen, H.-W. Kang, S.-Y. Hsiao, P.-F. Yang, K.-M. Chiang and H.-W. Lin, *Adv. Mater.*, 2014, **26**, 6647-6652.
8. J. You, Z. Hong, Y. Yang, Q. Chen, M. Cai, T.-B. Song, C.-C. Chen, S. Lu, Y. Liu, H. Zhou and Y. Yang, *ACS Nano*, 2014, **8**, 1674-1680.
9. Y. Xia, K. Sun, J. Chang and J. Ouyang, *J. Mater. Chem. A*, 2015, **3**, 15897-15904.
10. W. Nie, H. Tsai, R. Asadpour, J.-C. Blancon, A. J. Neukirch, G. Gupta, J. J. Crochet, M. Chhowalla, S. Tretiak, M. A. Alam, H.-L. Wang and A. D. Mohite, *Science*, 2015, **347**, 522-525.
11. Y. Xia and J. Ouyang, *J. Mater. Chem.*, 2011, **21**, 4927-4936.
12. D. Alemu, H.-Y. Wei, K.-C. Ho and C.-W. Chu, *Energy Environ. Sci.*, 2012, **5**, 9662-9671.
13. Z. Li, F. Qin, T. Liu, R. Ge, W. Meng, J. Tong, S. Xiong and Y. Zhou, *Org. Electron.*, 2015, **21**, 144-148.
14. Z.-K. Wang, M. Li, D.-X. Yuan, X.-B. Shi, H. Ma and L.-S. Liao, *ACS Appl. Mater.Interfaces*, 2015, **7**, 9645-9651.
15. Q. Chen, H. Zhou, Z. Hong, S. Luo, H.-S. Duan, H.-H. Wang, Y. Liu, G. Li and Y. Yang, *J. Am. Chem. Soc.*, 2013, **136**, 622-625.
16. P.-W. Liang, C.-Y. Liao, C.-C. Chueh, F. Zuo, S. T. Williams, X.-K. Xin, J. Lin and A. K. Y. Jen, *Adv. Mater.*, 2014, **26**, 3748-3754.
17. W. Li, K. H. Hendriks, A. Furlan, W. S. C. Roelofs, M. M. Wienk and R. A. J. Janssen, *J. Am. Chem. Soc.*, 2013, **135**, 18942-18948.
18. K. Sun, Y. Xia and J. Ouyang, *Sol. Energy Mater. Sol. Cells*, 2012, **97**, 89-96.
19. S. K. M. Jönsson, J. Birgerson, X. Crispin, G. Greczynski, W. Osikowicz, A. W. Denier van der Gon, W. R. Salaneck and M. Fahlman, *Synth. Met.*, 2003, **139**, 1-10.
20. X. Crispin, F. L. E. Jakobsson, A. Crispin, P. C. M. Grim, P. Andersson, A. Volodin, C. van Haesendonck, M. Van der Auweraer, W. R. Salaneck and M. Berggren, *Chem. Mater.*, 2006, **18**, 4354-4360.
21. G. Greczynski, T. Kugler, M. Keil, W. Osikowicz, M. Fahlman and W. R. Salaneck, *J. Electron Spectrosc. Relat. Phenom.*, 2001, **121**, 1-17.
22. W. Zhang, M. Saliba, D. T. Moore, S. K. Pathak, M. T. Hörantner, T. Stergiopoulos, S. D. Stranks, G. E. Eperon, J. A. Alexander-Webber, A. Abate, A. Sadhanala, S. Yao, Y. Chen, R. H. Friend, L. A. Estroff, U. Wiesner and H. J. Snaith, *Nat. Commun.*, 2015, **6**, 6142.
23. A. Abate, M. Saliba, D. J. Hollman, S. D. Stranks, K. Wojciechowski, R. Avolio, G. Grancini, A. Petrozza and H. J. Snaith, *Nano Lett.*, 2014, **14**, 3247-3254.
24. H. Zhou, Q. Chen, G. Li, S. Luo, T.-b. Song, H.-S. Duan, Z. Hong, J. You, Y. Liu and Y. Yang, *Science*, 2014, **345**, 542-546.
25. C. Sun, Z. Wu, H.-L. Yip, H. Zhang, X.-F. Jiang, Q. Xue, Z. Hu, Z. Hu, Y. Shen, M. Wang, F. Huang and Y. Cao, *Adv. Energy Mater.*, 2015, 201501534.
26. N. K. Noel, A. Abate, S. D. Stranks, E. S. Parrott, V. M. Burlakov, A. Goriely and H. J. Snaith, *ACS Nano*, 2014, **8**, 9815-9821.
27. C.-C. Chueh, C.-Y. Liao, F. Zuo, S. T. Williams, P.-W. Liang and A. K. Y. Jen, *J. Mater. Chem. A*, 2015, **3**, 9058-9062.

Solvent treatment effect of the PEDOT:PSS anode interlayer in inverted planar perovskite solar cells

Xue-Yuan Li, Lian-Ping Zhang, Feng Tang, Zhong-Min Bao, Jian Lin, Yan-Qing Li, Liwei Chen, Chang-Qi Ma

PSS-rich surface was found to be helpful in improving perovskite thin film quality, and the consequence device performance.